

Supplementary Information [SI] for

Purpose in life, neural alcohol cue reactivity, and daily alcohol use in social drinkers

Yoona Kang*, Danielle Cosme, David Lydon-Staley, Jeeseung Ahn, Mia Jovanova, Faustine Corbani, Silica Lomax, Ovidia Stanoi, Victor Strecher, Peter J. Mucha, Kevin Ochsner, Dani S. Bassett & Emily B. Falk*

*Corresponding authors

yoona.kang@asc.upenn.edu, emily.falk@asc.upenn.edu

Notes: Data and analysis scripts are available in https://github.com/cnlab/purpose_craving.

S1. Recruitment and participant sample characteristics

College students who belonged to undergraduate campus groups at the time of recruitment were invited to participate. First, we identified campus groups across two universities through flyers, university websites, in-person information sessions, and email communications. A group was determined to be eligible if: 1) it had at least 15 members, 2) members reported having social interactions on a regular basis, and 3) at least 80% of the members were interested in participating. This group-based sampling method was a part of a larger parent study that examined social influences on health behavior. Of the 583 initial participants across 24 campus groups who consented and completed an online survey, 111 consenting participants who met the functional magnetic resonance imaging (fMRI) eligibility criteria based on their self-reports completed an fMRI visit and had usable data. Eligibility criteria for the fMRI visit included standard MRI eligibility criteria (no metal in body, not claustrophobic, not pregnant or nursing, and weighs less than 350lb due to weight limit of the fMRI scanner), older than 18 years of age, fluent in English, having no history of serious medical history, psychiatric hospitalization, or drug abuse, and not currently studying abroad. Given the focus of the current study on alcohol use outcomes, participants were excluded if they had a history of alcohol abuse, never drank alcohol in their life, or consumed less than one drink in a typical drinking occasion. As part of a parent study, additional eligibility included having at least two friends who drink more and two who drink less than the self.

All participants who completed fMRI were invited to an initial round of ecological momentary assessment (EMA) that did not contain the purpose in life question, hence was not used in the current report. About nine months (mean=307.8 days, median=280 days; $SD=135.75$, range=85-533) after the fMRI scan, at the start of the coronavirus disease 2019 (COVID-19) pandemic, all participants were once again invited to complete an additional 28-day EMA, which included the purpose in life measure relevant to the current investigation. Of the initial participants who completed the fMRI visit, 54 participants also completed the EMA portion of the study with usable data (mean_{age}=20.35 years, $SD_{age}=1.32$; 37 women; 26 White, 16 Asian, 3 Hispanic, 2 Black, 7 Others). Demographic variables were not associated with any of the main study variables ($p>.10$), with an exception that men compared to women and other genders

showed greater alcohol cue reactivity within the ventral striatum, $F(2,51)=3.191$, $p=.050$. All analyses controlled for demographic variables (age, gender, race/ethnicity, and social status); all results remained parallel when we did not control for demographic variables [S6].

S2. Alcohol cue reactivity fMRI task, preprocessing, and modeling

During the fMRI appointment, participants completed an alcohol cue reactivity task, which has been previously used to identify neural regions responsive to alcohol cues.^{1,2} All participants completed 96 trials of different trial types across four task runs. The current report includes results from trials during which participants were instructed to “react naturally” to images of alcohol (24, 32, or 48 trials depending on the between-subject condition assignment as part of a larger parent study). Specifically, participants were instructed:

“One way of experiencing pictures of alcohol is to simply look at them and respond according to your initial gut reaction. For example, if you see a picture of beer, you can simply look at it and react naturally, without thinking of anything in particular. So, when you see the word REACT, just look at the picture and react naturally.”

During these trials, participants were presented with images of beer, wine, and liquor³ and asked to “simply look at them and respond according to your initial gut reaction,” followed by indicating their craving rated on a 1 (*not at all*) to 5 (*very much*) scale (craving scores not reported here). Other trials that were not the focus of the current report included viewing images of non-alcoholic beverages and (up/down) regulating craving in response to alcohol images. Each block consisted of 4 trials and began with a trial condition cue (3s) followed by 4 trials, each consisting of an image presentation (6s) and a craving rating (3s). Each event was separated by a jittered fixation cross (mean=4.0s, $SD=2.6s$).

The structural and task-based fMRI scans were preprocessed using fMRIPrep⁴ (Version 20.0.6), which is based on Nipype 1.4.2^{5,6}. The T1-weighted (T1w) image was corrected for intensity non-uniformity (INU) with N4BiasFieldCorrection,⁷ distributed with ANTs 2.2.0⁸, and used as T1w-reference throughout the workflow. The T1w-reference was then skull-stripped with a Nipype implementation of the ANTs brain extraction workflow, using OASIS30ANTs as target template. Brain tissue segmentation of cerebrospinal fluid (CSF), white-matter (WM) and gray-matter (GM) was performed on the brain-extracted T1w using fast (FSL 5.0.9⁹). Brain surfaces were reconstructed using recon-all (FreeSurfer 6.0.1¹⁰), and the brain mask estimated previously was refined with a custom variation of the method to reconcile ANTs-derived and FreeSurfer-derived segmentations of the cortical gray-matter of Mindboggle.¹¹ Volume-based spatial normalization to one standard space (MNI152NLin2009cAsym¹²) was performed through nonlinear registration with antsRegistration (ANTs 2.2.0), using brain-extracted versions of both T1w reference and the T1w template.

For functional blood oxygen level dependent (BOLD) scans, the following preprocessing was performed. First, a reference volume and its skull-stripped version were generated using a custom methodology of fMRIPrep. A B0-nonuniformity map (or fieldmap) was estimated based on two echo-planar imaging (EPI) references with opposing phase-encoding directions, with 3dQwarp¹³ with AFNI 20160207. Based on the estimated susceptibility distortion, a corrected

EPI reference was calculated for a more accurate co-registration with the anatomical reference. The BOLD reference was then co-registered to the T1w reference using `bbregister` from FreeSurfer, which implements boundary-based registration.¹⁴ Co-registration was configured with six degrees of freedom. Head-motion parameters with respect to the BOLD reference (transformation matrices, and six corresponding rotation and translation parameters) are estimated before any spatiotemporal filtering using `mcflirt` (FSL 5.0.9).¹⁵ BOLD runs were slice-time corrected using `3dTshift` from AFNI 20160207.¹³ The BOLD time-series were resampled onto their original, native space by applying a single, composite transform to correct for head-motion and susceptibility distortions. The BOLD time-series were resampled into standard space, generating a preprocessed BOLD run in MNI152Nlin2009cAsym space. All resamplings were performed with a single interpolation step by composing all the pertinent transformations (i.e. head-motion transform matrices, susceptibility distortion correction when available, and co-registrations to anatomical and output spaces). Gridded (volumetric) resamplings were performed using `antsApplyTransforms` (ANTs), configured with Lanczos interpolation to minimize the smoothing effects of other kernels.¹⁶ Non-gridded (surface) resamplings were performed using `mri_vol2surf` (FreeSurfer). Various confounds (e.g., framewise displacement, DVARS, global signal) were also calculated for each TR and logged in a confounds file (for additional details, see <https://fmriprep.org/en/20.0.6/outputs.html#confounds>). The outputs from fMRIPrep were then manually quality checked to ensure adequate preprocessing.

Prior to first-level modeling, we generated motion regressors using an automated motion assessment tool¹⁷ (<https://github.com/dcosme/auto-motion-fmriprep>). This tool is a predictive model that utilizes the confound files generated by fMRIPrep and classifies whether or not fMRI volumes contain motion artifacts. The classifier is applied to each participant's task run and returns a binary classification indicating the presence or absence of motion artifacts for each volume. In addition, this tool transforms the realignment parameters into Euclidean distance for translation and rotation separately, and calculates the displacement derivative of each. This yields a total of five motion regressors for first-level modeling.

Participants completed four runs of the cue reactivity task (460 volumes in total). The cue reactivity task was modeled including the following regressors of interest for trial condition cue, modeled as the 6s period during image presentation: react naturally to alcohol cues, react naturally to non-alcohol cues, downregulate response to alcohol cues, and upregulate response to alcohol cues. Models also included the following nuisance regressors not of interest: rating period and five motion regressors mentioned above (<https://github.com/dcosme/auto-motion-fmriprep>). Realignment parameters were transformed into Euclidean distance for translation and rotation separately, and we included the displacement derivative of each. Another "trash" regressor marked images with motion artifacts (e.g., striping) identified via automated motion assessment¹⁷ and visual inspection. Individual task runs were excluded for having >10% of volumes contaminated with motion artifacts, which was more than 23 *SD* from the median (median=0.0%, *SD*=0.4%). This resulted in all of one participant's data being excluded.

All data were high-pass filtered at 128 seconds and temporal autocorrelation was modeled using the FAST method.¹⁸ To index cue reactivity to alcohol, we extracted mean parameter estimates

from the react naturally to alcohol cues > rest contrast within the ventral striatum region of interest (ROI). The ventral striatum ROI was taken from a meta-analysis of 206 studies that reported neural signals associated with reward/positive value processing.¹⁹ This resulted in a single value per participant that was used as an individual difference measure of alcohol cue reactivity in subsequent analyses. In addition, a meta-analytically defined map of craving-related activity was extracted from the online database Neurosynth (www.neurosynth.org)²⁰ using the search term 'craving' (80 studies; using Neurosynth's default threshold $p < .01$, corrected). Please see S3 below for results using the neural activity within the reverse inference map of 'craving.'

S3. Ecological momentary assessment (EMA) data collection and transformation

Throughout the 28-day EMA period, participants received two surveys per day via mobile app in the morning (8am) and evening (6pm) that assessed current levels of purpose in life (morning only) and alcohol-related questions (morning and evening). To minimize participant burden in the context of the larger study from which these data were drawn, participants received the purpose in life prompt once per day. Given that the major focus of the main study was on alcohol-related behavior, participants received alcohol-related prompts (craving, consumption) twice per day.

We transformed time-varying variables (purpose, alcohol craving, alcohol consumption) as follows: First, to account for the zero-inflated data (i.e., alcohol consumption) and to focus on within-person relationships (e.g., comparing times when people feel a stronger vs. weaker sense of purpose), time-varying variables were within-person standardized to z scores, which allowed us to test within-person changes while holding the between-person differences constant. Following standardization, 0 on these time-varying variables indicated occasions of typical purpose, alcohol craving, and alcohol consumption for each individual, values above 0 indicated occasions of higher than usual and values below 0 indicated occasions of lower than usual purpose, alcohol craving, and alcohol consumption for each participant. Standardization also removed participants who reported no drinking throughout the EMA period (i.e., zero variability in number of drinks). Second, to test the lagged associations, the morning levels of purpose in life were first carried forward to the same day's evening ratings to indicate an average level of purpose in life on each day. We then created previous moment's craving and purpose in life variables by lagging them by one prompt level. The lagged models thus included alcohol craving at a previous point and/or daily purpose in life at a previous time as predictors of alcohol consumption reported at a later time point.

As noted in the main text, the purpose ("Right now, I feel that I have a sense of direction and purpose in my life") and the craving ("How strongly are you craving alcohol right now?") measures assessed participants' present states *in situ*, whereas the alcohol consumption measure asked aggregate amounts since the last survey ("Since your morning/evening survey, have you consumed any alcohol?"). This lagged design thus tested whether 1) craving and purpose ratings from the morning predicted alcohol consumption from morning till afternoon,

and 2) purpose from morning and craving from evening predicted alcohol consumption from evening till next morning (Table S3).

Missing data were present at level-1 variables, including two predictor (craving=616 [20.37% missing], purpose=495 [32.74% missing]) and one outcome (drinking amount=1042 [34.46% missing]) variables out of 3024 (craving, drinking amount) and 1512 (purpose) total possible data points. Missing data were handled by row-wise deletion.

Table S3. Lagged EMA model

	day 0	day1		day2		day 3
Unlagged						
Purpose		day1 morning		day2 morning		
Craving		day1 morning	day1 evening	day2 morning	day2 evening	
Alcohol consumption		day0 evening/night	day1 morning/afternoon	day1 evening/night	day2 morning/afternoon	day2 evening/night
Lagged						
Purpose			day1 morning		day2 morning	
Craving			day1 morning	day1 evening	day2 morning	day2 evening
Alcohol consumption		day0 evening/night	day1 morning/afternoon	day1 evening/night	day2 morning/afternoon	day2 evening/night
Purpose carried forward (The final model in the current report)						
Purpose			day1 morning	day1 morning	day2 morning	day2 morning
Craving			day1 morning	day1 evening	day2 morning	day2 evening
Alcohol consumption		day0 evening/night	day1 morning/afternoon	day1 evening/night	day2 morning/afternoon	day2 evening/night

S4. Neurosynth map of ‘craving’

We repeated the multilevel analyses that examined the relationships among neural reactivity to alcohol cues, purpose in life, craving, and subsequent alcohol use using the neurosynth map of ‘craving.’ Neurosynth automatically synthesizes published fMRI data (507891 activations reported in 14371 studies as of October 2021). Using meta-analytic procedures, Neurosynth allows the users to search common activation patterns during psychological states with representational search terms. Neural signature of craving (i.e., regions associated with craving processing for reverse inferences) was derived from the search term ‘craving’ (80 studies; using Neurosynth’s default threshold $p < .01$, corrected), which included clusters in the ventral striatum and anterior cingulate cortex that extended to the ventromedial prefrontal cortex (<https://neurosynth.org/analyses/terms/craving/>).

Paralleling our main results that focused on ventral striatum activity, in our non-dependent social drinker sample, viewing alcohol images did not lead to significant increases in activity from rest within the neurosynth map of craving ($t(53)=0.037$, $p=0.970$), consistent with previous work that showed greater craving among alcohol-dependent vs. social drinkers.²¹ Further, there was a significant three-way interaction when we tested daily purpose in life, alcohol cue reactivity within the neurosynth map of craving, alcohol craving, and their interaction terms simultaneously as predictors of subsequent alcohol use ($b=-0.133$, $p=.017$; Table SI). Follow-up simple slopes analysis examined whether neural reactivity to alcohol cues within the neurosynth map of craving interacted with daily craving to predict subsequent alcohol use across different levels of daily purpose in life. Although these interactions were not significant at each level of purpose, the relationship was stronger at lower ($b=0.015$, $p=.121$), compared to mean ($b=0.010$, $p=.298$), or higher levels of daily purpose ($b=0.00%$, $p=.612$). (Figure SI)

Table S4. Multilevel analyses of alcohol craving, neural reactivity to alcohol cues within the meta-analytically defined Neurosynth map of ‘craving’, and purpose in daily life predicting the amount of alcohol consumed.

	β	b	se	t	p	95% CI	d
Craving	0.212	0.212	0.051	4.166	<0.001	0.112, 0.312	1.504
Purpose in life	0.031	0.031	0.026	1.181	0.238	-0.020, 0.082	0.065
Neurosynth map of craving	-0.043	-0.080	0.058	-1.398	0.162	-0.193, 0.032	-0.077
Craving * Purpose in life	0.005	0.005	0.026	0.194	0.847	-0.046, 0.057	0.011
Craving * Neurosynth map of craving	-0.009	-0.018	0.098	-0.179	0.859	-0.210, 0.174	-0.065
Purpose in life * Neurosynth craving	-0.050	-0.093	0.050	-1.874	0.061	-0.190, 0.004	-0.103
Craving * Purpose in life * Neurosynth map of craving	-0.066	-0.133	0.056	-2.379	0.017	-0.243, -0.024	-0.130

Notes: Standardized (β) and unstandardized (b) regression coefficients, 95% confidence intervals (CI), standard error for unstandardized regression coefficients (se), and Cohen’s *d* scores (d) are displayed. Time-varying variables (purpose in life, alcohol craving, and amount of later alcohol consumption) were within-person standardized (N=54; 1358 observations). All analyses controlled for potential covariates, including demographic variables (age, gender, race/ethnicity, and perceived social status) and the condition assignment as part of a parent study. Please see https://github.com/cnlab/purpose_craving for the complete model output statistics. The phrase “Neurosynth map of craving” indicates the neural reactivity to alcohol cues, while naturally reacting to images of alcoholic beverages, within the meta-analytically defined regions associated with craving processing, derived from the search term ‘craving’ in neurosynth.org.

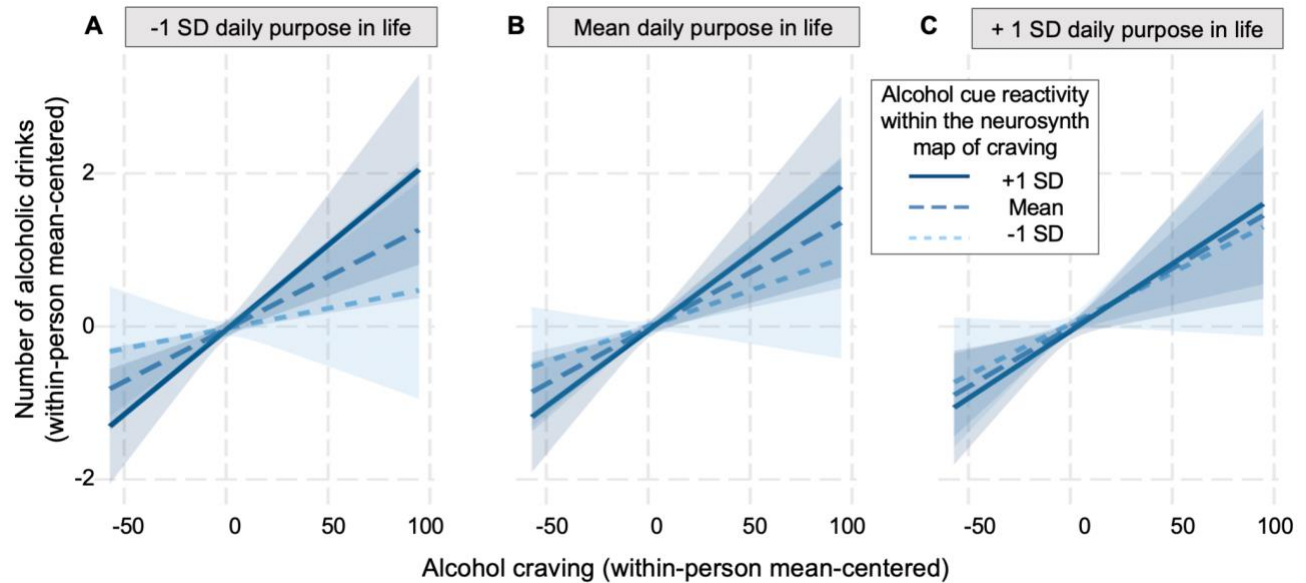


Figure S4. Simple slopes analyses examining whether alcohol cue reactivity within the neurosynth map of ‘craving’ interacted with daily craving to predict alcohol use across three levels of purpose in life. Although interactions were not significant at any level of purpose, this relationship was stronger at lower (A), compared to mean (B) or higher (C) levels of daily purpose.

S5. Multilevel regression model fit and test of multicollinearity

The three-way interaction model (craving * ventral striatum * purpose) showed better model fit (Akaike information criterion [AIC]=3735.7), compared to separate two-way interaction models, including the craving * ventral striatum (AIC=3830.8), purpose * vs (AIC=3830.8), and craving * purpose (AIC=3743.0). Chi-squared test further showed that the three-way interaction model significantly improved fit over the craving * purpose model that had the lowest AIC among the two-way interaction models ($\chi^2(1)=15.326$, $p=0.004$). We detected no issues of multicollinearity (Variance Inflation Factor [VIF] mean=1.050, range=1.013-1.079). The simple slopes analysis results were robust to False Discovery Rate (FDR) correction (FDR-adjusted p values for craving * ventral striatum interactions at lower (.045), mean (.109), and higher (.320) levels of purpose).

S6. Results not controlling for potential covariates

We repeated analysis without controlling for potential covariates, including the demographic variables (age, gender, race/ ethnicity, and perceived social status within a campus group) and the condition assignment as part of a larger study. All results remained parallel: Craving alcohol more at a previous time point was associated with consuming a larger amount of alcohol at a later time point ($b=0.201$, $p<.001$). We also found a significant three-way interaction ($b=-0.074$, $p=.003$), and follow-up simple slopes analyses showed that alcohol cue reactivity within the

ventral striatum strengthened the link between alcohol craving and the subsequent amount of consumption only when people were previously feeling weaker ($b=0.010$, $p=.022$) levels of daily purpose. By contrast, when people were previously at their mean ($b=0.008$, $p=.052$) or higher ($b=0.006$, $p=.138$) than their usual levels of daily purpose, neural alcohol cue reactivity did not affect the relationship between alcohol craving and the subsequent amount of consumption.

S7. An interaction between daily purpose in life and ventral striatum activity predicting subsequent alcohol use.

When we examined daily purpose in life and neural reactivity to alcohol cues within the ventral striatum as potential moderators in the link between alcohol craving and subsequent amount of alcohol consumption, we found a significant two-way interaction between daily purpose in life and ventral striatum activity predicting subsequent alcohol use, which we reported in the main text ($b=-0.053$, $p=.031$). Follow-up simple slopes analyses revealed no significant direct associations between ventral striatum activity and alcohol consumption across different levels of purpose in life, but the relationship between ventral striatum activity and alcohol use was directionally positive at lower levels of purpose ($b=0.023$, $p=.468$), whereas it was negative at higher levels of purpose in life ($b=-0.047$, $p=.146$).

S8. Results controlling for the number of days between the fMRI and EMA data collection.

We repeated analysis controlling for the number of days between the fMRI visit and the first day of EMA data collection. The number of days was not associated with any of the main predictor or outcome variables ($ps>.20$). All results reported in the main text remained parallel: Craving alcohol more at a previous time point was associated with consuming a larger amount of alcohol at a later time point ($b=0.209$, $p<.001$). We also found a significant three-way interaction ($b=-0.087$, $p<.001$), and follow-up simple slopes analyses showed that alcohol cue reactivity within the ventral striatum strengthened the link between alcohol craving and the subsequent amount of consumption only when people were previously feeling lower than their usual levels of daily purpose ($b=0.012$, $p=.015$). By contrast, when people were previously at their mean ($b=0.008$, $p=.071$) or higher ($b=0.005$, $p=.319$) than their usual levels of daily purpose, neural alcohol cue reactivity did not affect the relationship between alcohol craving and the subsequent amount of consumption.

Supplementary Information References

1. Schacht, J. P., Anton, R. F. & Myrick, H. Functional neuroimaging studies of alcohol cue reactivity: a quantitative meta-analysis and systematic review. *Addict. Biol.* 18, 121–133 (2013).
2. Hill-Bowen, L. D. *et al.* The cue-reactivity paradigm: An ensemble of networks driving attention and cognition when viewing drug and natural reward-related stimuli. *bioRxiv* 2020.02.26.966549 (2021) doi:10.1101/2020.02.26.966549.
3. López-Caneda, E. & Carbia, C. The Galician Beverage Picture Set (GBPS): A standardized database of alcohol and non-alcohol images. *Drug Alcohol Depend.* 184, 42–47 (2018).
4. Esteban, O. *et al.* fMRIPrep: a robust preprocessing pipeline for functional MRI. *Nat. Methods* 16, 111–116 (2019).
5. Gorgolewski, K. *et al.* Nipype: a flexible, lightweight and extensible neuroimaging data processing framework in python. *Front. Neuroinform.* 5, 13 (2011).
6. Gorgolewski, K. J. *et al.* Nipype. *Software. Zenodo.* <https://doi.org/10.5281/zenodo.596855>, (2018).
7. Tustison, N. J. *et al.* N4ITK: improved N3 bias correction. *IEEE Trans. Med. Imaging* 29, 1310–1320 (2010).
8. Avants, B. B., Epstein, C. L., Grossman, M. & Gee, J. C. Symmetric diffeomorphic image registration with cross-correlation: evaluating automated labeling of elderly and neurodegenerative brain. *Med. Image Anal.* 12, 26–41 (2008).
9. Zhang, Y., Brady, M. & Smith, S. Segmentation of brain MR images through a hidden Markov random field model and the expectation-maximization algorithm. *IEEE Trans. Med. Imaging* 20, 45–57 (2001).
10. Dale, A. M., Fischl, B. & Sereno, M. I. Cortical surface-based analysis. I. Segmentation and surface reconstruction. *Neuroimage* 9, 179–194 (1999).
11. Klein, A. *et al.* Mindboggling morphometry of human brains. *PLoS Comput. Biol.* 13, e1005350 (2017).
12. Fonov, V. S., Evans, A. C., McKinstry, R. C., Almlí, C. R. & Collins, D. L. Unbiased nonlinear average age-appropriate brain templates from birth to adulthood. *Neuroimage Supplement* 1, S102 (2009).
13. Cox, R. W. & Hyde, J. S. Software tools for analysis and visualization of fMRI data. *NMR in Biomedicine* vol. 10 171–178 (1997).
14. Greve, D. N. & Fischl, B. Accurate and robust brain image alignment using boundary-based registration. *Neuroimage* 48, 63–72 (2009).
15. Jenkinson, M., Bannister, P., Brady, M. & Smith, S. Improved optimization for the robust and accurate linear registration and motion correction of brain images. *Neuroimage* 17, 825–841 (2002).
16. Lanczos, C. Evaluation of Noisy Data. *Journal of the Society for Industrial and Applied Mathematics Series B Numerical Analysis* 1, 76–85 (1964).
17. Cosme, D., Flournoy, J. C. & Vijayakumar, N. auto-motionfmriprep: A tool for automated assessment of motion artifacts. *Zenodo DOI* 10, (2018).
18. Corbin, N., Todd, N., Friston, K. J. & Callaghan, M. F. Accurate modeling of temporal correlations in rapidly sampled fMRI time series. *Hum. Brain Mapp.* 39, 3884–3897 (2018).
19. Bartra, O., McGuire, J. T. & Kable, J. W. The valuation system: a coordinate-based meta-

analysis of BOLD fMRI experiments examining neural correlates of subjective value. *Neuroimage* 76, 412–427 (2013).

20. Yarkoni, T., Poldrack, R. A., Nichols, T. E., Van Essen, D. C. & Wager, T. D. Large-scale automated synthesis of human functional neuroimaging data. *Nat. Methods* 8, 665–670 (2011).
21. Naqvi, N. H. *et al.* Cognitive Regulation of Craving in Alcohol-Dependent and Social Drinkers. *Alcoholism: Clinical and Experimental Research* vol. 39 343–349 (2015).